Boundary-Condition Quantum Mechanics IV_b: Baseline inertial-noise spectra from a W_coh-blind event-chain control model

Peter M. Ferguson
Independent Researcher

5th December 2025

Abstract

This follow-up to the BCQM inertial-noise programme [1, 2] develops a minimal, simulation-based account of the inertial acceleration-noise spectrum associated with discrete event chains. Building on the primitives and scaling hypotheses of BCQM III and BCQM IV [3, 1], we define a simple BCQM-compatible, W_{coh}-blind control model for a single probe world-line (a point-mass degree of freedom) and use it to generate dimensionless spectra $S_a(\omega; W_{\mathrm{coh}})$ over a range of coherence horizons W_{coh}. We examine the existence and qualitative shape of these spectra, test whether they collapse onto a universal form when plotted as $S_a(\omega; W_{\mathrm{coh}})/A_a(W_{\mathrm{coh}})$ against the natural dimensionless frequency $\omega\Delta t$, and extract an effective scaling exponent $A_a(W_{\mathrm{coh}}) \propto W_{\mathrm{coh}}^{-\beta}$. For this minimal control kernel the inferred exponent is consistent with $\beta = 0$, as expected for dynamics in which W_{coh} does not enter the microscopic update rule. Validation against toy models confirms that the pipeline accurately recovers scaling when present, ensuring the null result is physical.

We then convert the dimensionless results into SI units for representative mechanical and atomic benchmark platforms, obtaining baseline order-of-magnitude estimates for the BCQM inertial noise floor and the corresponding thermal crossover temperature T_{crit}, understood as functions of the chosen physical time and length scales. Finally, we introduce a simple independent-probe cluster toy in configuration space to compare the centre-of-mass spectra of single probes and finite clusters, using this as a baseline protocol for testing few-body suppression of BCQM inertial noise and laying groundwork for more realistic correlated cluster models and for the emergent-curvature analysis in BCQM V.

1 Introduction and scope

Boundary-Condition Quantum Mechanics (BCQM) proposes that inertial motion and spacetime structure emerge from stochastic chains of discrete quantum events, rather than being imposed *a priori* as a smooth background. The first BCQM papers established the basic two-axis picture, the role of a finite coherence horizon W_{coh}, and a graph-based dynamics for probability amplitudes [4, 5, 6]. BCQM III and BCQM IV, in particular, outlined how an effective inertial response and an associated acceleration-noise floor can arise from fluctuations in these event chains [3, 1, 2].

The present follow-up paper focuses on a limited and concrete part of that programme: the inertial acceleration-noise spectrum associated with a single probe world-line and with small bound clusters. Our goals are to exhibit and characterise the dimensionless spectra $S_a(\omega; W_{\mathrm{coh}})$ for a minimal BCQM-compatible model, to test simple scaling and universality hypotheses as the coherence horizon is varied, to translate the resulting noise levels into SI units for representative mechanical and atomic benchmarks, and to explore how the noise is modified for few-body clusters.

Equally important is what this paper does *not* attempt to do. We do not design or analyse specific experiments in detail, we do not introduce the gravitational sector, and we do not claim to deliver the full phenomenology planned for BCQM V. The scope here is deliberately modest: to provide a first quantitative account of BCQM inertial noise spectra in simple settings, and to supply a small number of well-defined numbers and scaling laws that can be carried forward into later work.

Related work. There is a substantial literature on objective-collapse and stochastic modifications of quantum mechanics, including the GRW family of models and continuous-spontaneous-localisation (CSL) dynamics that introduce explicit stochastic terms to generate mass-proportional noise and suppress macroscopic superpositions [7, 8]. In the present BCQM programme the focus is different: an intrinsic coherence horizon W_{coh} is introduced at the level of the underlying event dynamics (see Sec. 2 and Refs. [9, 3]), and ordinary environmental decoherence is treated as an additional effect to be layered on top of this horizon rather than as its origin. The numerical studies in this paper deliberately restrict attention to a W_{coh}-blind control kernel, so that any future detection of W_{coh}-dependent inertial-noise amplitudes in more physical BCQM models can be attributed to their hop statistics rather than to ad hoc collapse terms.

2 Minimal BCQM-compatible model for inertial noise

We work with a deliberately simple BCQM-compatible model that stays as close as possible to the primitives already used in BCQM III. The basic object is a directed event graph whose vertices represent realised events and whose edges carry complex amplitudes. At each discrete time step a hop-bounded kernel selects a neighbourhood of vertices within a fixed hop radius, and the corresponding amplitudes define the local propensity for the next event along a given world-line.

Framing assumptions. The discrete hop model used in this section is deliberately minimal, but it is not arbitrary. It is constrained by four requirements that reflect the pre-spacetime BCQM picture and the known properties of emergent spacetime:

- *Locality.* Each hop uses only local information: the current realised event and the immediately preceding one. This defines a "rudder" (the last displacement) which tilts, but does not fix, the probability distribution for the next event.
- *Symmetry.* The underlying 1D chain carries no absolute notion of "left" or "right". The hop kernel is symmetric under relabelling of the chain and reversal of the rudder. Only the *relative* direction "I was there, now I am here" is meaningful.
- *No background bath.* At the primitive level there is no electromagnetic or gravitational environment that continuously damps a wavefunction. The only changes to the effective state of the particle are due to its own hops and occasional interruptions from other events or threads. We therefore avoid GKLS-style damping [10, 11] and instead use a simple "rudder + interruption" rule.
- *Single intrinsic horizon.* The coherence horizon W_{coh} appears only as a single intrinsic timescale controlling the typical separation between interruptions of the rudder-guided motion. Short W_{coh} leads to frequent interruptions and jagged trajectories; long W_{coh} leads to long, nearly straight runs. No additional background scales are introduced at this level: in the numerical implementation W_{coh} is measured in units of hops and the basic time step Δt is the hop time, so combinations such as $\omega\Delta t$ used below are natural dimensionless frequency variables.

Under these constraints, we model the local q-wave propensity for the next hop conceptually as a smooth "bow" of directions centred on the rudder. In the present paper we work with the simplest 1D discretisation of this picture: the probe moves on a nearest-neighbour chain, and the bow reduces to a hop to the left or right neighbour with a small rudder-dependent bias. Occasional interruptions, with a mean separation set by W_{coh}, temporarily restore an unbiased hop and represent the coarse-grained influence of other events or threads. The realised event at each tick is a single stochastic sample from this discrete bow. The explicit 1D update rule used in the numerics is given in Appendix A, and the resulting trajectories yield an intrinsic inertial noise amplitude $A(W_{\mathrm{coh}})$.

Within this event network we focus on a single realised chain of events, treating its world-line as a probe of the underlying propensity structure. We interpret this probe world-line as a point-mass degree of freedom and use its discrete trajectory to define an effective position and acceleration as functions of a discrete simulation-time parameter. An effective reference frame for the probe is fixed by the underlying drift of the event chain: we choose coordinates in which the mean probe world-line is straight and uniform. In what follows, we loosely refer to this as an 'inertial frame' for the BCQM simulation, although it is defined operationally from the event statistics rather than assumed a priori. This facilitates measuring accelerations relative to a nominally straight world-line in the absence of noise.

The coherence horizon W_{coh} enters through a simple phase-memory rule: amplitudes contributing to the hop kernel are damped beyond a time window of order W_{coh}, so that phase correlations decay on that scale. In the limit of large W_{coh} the probe experiences long-range temporal correlations along its world-line, whereas for small W_{coh} the noise approaches a more local, memoryless regime. The remainder of the paper uses this minimal model as the basis for generating inertial acceleration-noise spectra and studying their scaling behaviour.

3 Numerical method and diagnostics

The inertial-noise spectra in this paper are obtained from ensembles of discrete probe trajectories generated on the event graph. Each simulation run produces a time series for the probe position in this reference frame, from which we construct a discrete acceleration signal. We then form an estimate of the one-sided acceleration-noise spectrum $S_a(\omega)$ by applying standard time-series tools (windowing, Fourier transforms, and averaging over many realisations) with checks that the result is stable against reasonable variations of numerical parameters.

In this companion paper BCQM IV_b we specialise to a minimal, W_{coh}-blind control kernel on a single thread, implemented in the code package `bcqm_toy_3`; its precise update rule and the additional validation toys are summarised in Appendix A. Rather than implementing the full "rudder + interruption" hop model of section 2 in all its detail, we work with an effective single-thread Ornstein–Uhlenbeck–type acceleration kernel that reproduces its qualitative statistics while deliberately removing any explicit W_{coh} dependence. This ensures that any apparent W_{coh}-scaling seen in subsequent studies can be traced to the microdynamics of more BCQM-faithful kernels rather than to the control model itself. The full implementation, including the configuration files used for the figures in this paper, is available as an open companion code release on Zenodo [12].

To ensure that the spectra reflect genuine features of the BCQM model rather than numerical artefacts, we monitor a small set of diagnostics. These include basic consistency checks on the drift and variance of the probe motion, convergence tests with respect to the number and duration of trajectories, and simple conservation tests inherited from the underlying graph dynamics. Uncertainties on spectral amplitudes and fitted exponents are estimated from variations across independent runs and from the residuals of the fitting procedures. Further

algorithmic details, including the archived toy models and the canonical W_{coh}-blind control implementation `bcqm_toy_3` used here, are collected in Appendix A, together with parameter tables and additional convergence tests. The corresponding implementation is maintained in a dedicated version-controlled repository (BCQM_IV_b) and is publicly available together with the final BCQM IV_b release and its Zenodo companion record.

4 Results: spectra and scaling with the coherence horizon

We begin by presenting representative dimensionless spectra $S_a(\omega; W_{\mathrm{coh}})$ for a small set of coherence horizons W_{coh}, chosen to span the regime from relatively short to relatively long phase memory. For each W_{coh} we show the acceleration-noise spectrum obtained from the numerical procedure of section 3, together with a brief description of its qualitative features (low-frequency behaviour, any visible roll-off, and the absence or presence of strong numerical artefacts). Representative examples are shown in Fig. 1.

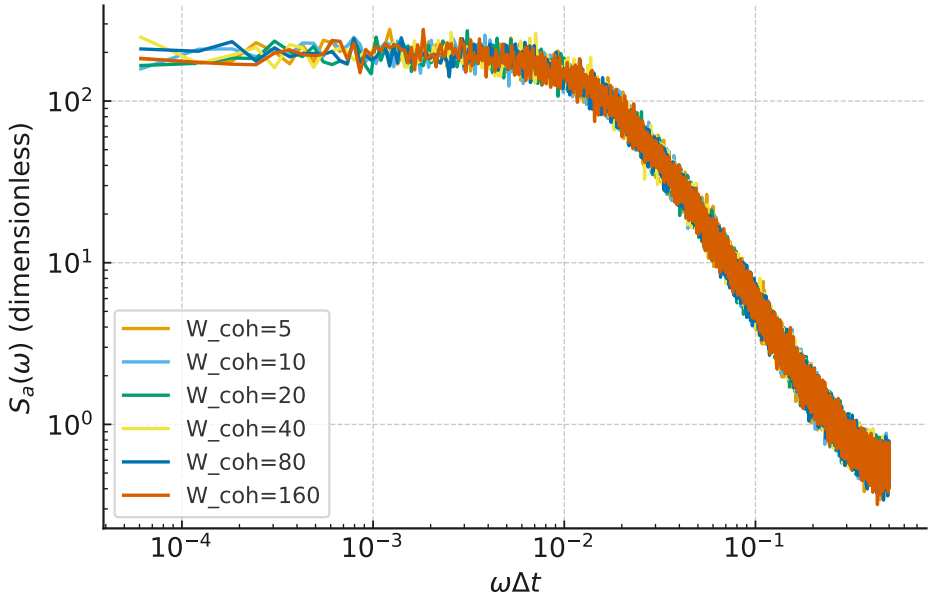

Figure 1: Dimensionless acceleration-noise spectra $S_a(\omega; W_{\mathrm{coh}})$ for the canonical W_{coh}-blind control kernel, shown for several coherence horizons W_{coh}. The curves are obtained from ensembles of trajectories generated by `bcqm_toy_3` using the numerical procedure of section 3. The spectra are smooth and display only very weak variation with W_{coh} over the scanned range, consistent with the control kernel being effectively W_{coh}-blind at the level of spectral shape.

Unless otherwise stated, all spectra and scaling results in this section are obtained from the canonical W_{coh}-blind control kernel implemented in the package `bcqm_toy_3` (see Appendix A).

From these spectra we extract an overall amplitude $A_a(W_{\mathrm{coh}})$ using a simple and explicitly stated convention (for example, a reference frequency in the flat part of the spectrum or an integrated band power), and we fit the dependence $A_a(W_{\mathrm{coh}}) \propto W_{\mathrm{coh}}^{-\beta}$. Figure 2 shows the resulting log–log plot of $A_a(W_{\mathrm{coh}})$ versus W_{coh}, together with the best-fit power-law trend. The quoted value of β and its uncertainty are obtained from standard fitting diagnostics and serve as a first quantitative test of the scaling hypothesis put forward in BCQM IV for the particular control kernel studied here; see Appendix A for details of the regression method and uncertainty estimates.

Finally, we perform a minimal universality test by rescaling the spectra to $S_a(\omega; W_{\mathrm{coh}})/A_a(W_{\mathrm{coh}})^2$ and plotting them against the dimensionless frequency $\omega\Delta t$. For the canonical W_{coh}-blind

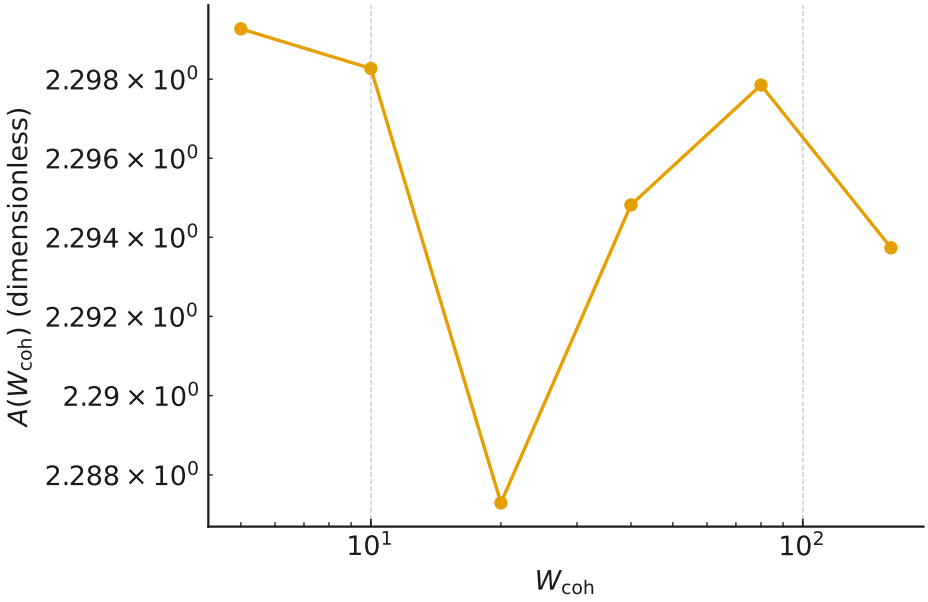

Figure 2: Dimensionless inertial-noise amplitude $A(W_{\mathrm{coh}})$ extracted from the spectra in Fig. 1, plotted as a function of the coherence horizon W_{coh} on log–log axes. Across the range $W_{\mathrm{coh}} = 5$–160 the amplitudes vary by less than 1 % around $A \approx 2.3$, and the fitted exponent β is consistent with zero. Together these observations confirm that the canonical control kernel is effectively W_{coh}-blind at the level of the overall noise amplitude.

control kernel the resulting curves show a reasonable but not perfect collapse: over the band $0.01 \leq \omega\Delta t \leq 0.3$, chosen to lie well above the lowest-frequency binning artefacts and well below the lattice cutoff, the rescaled spectra remain within 10–20 % of one another, with larger deviations confined to the high-frequency region near the lattice cutoff $\omega \sim 1/\Delta t$ where discretisation effects dominate. This behaviour is illustrated in Fig. 3 and is consistent with the view that the overall spectral shape is largely insensitive to W_{coh} for this minimal kernel, while leaving room for more structured behaviour in future W_{coh}-dependent models.

5 Results: SI units and experimental benchmarks

We now translate the dimensionless spectra into SI units for a small set of representative benchmark platforms. For illustration we focus on two broad classes: a mechanical resonator (such as a micron-scale oscillator) and a light-mass probe (for example a cold-atom interferometer), choosing mass scales and characteristic time-scales that are representative of existing or near-future experiments.

For each benchmark we map the simulation parameters $(\Delta t, \Delta x, W_{\mathrm{coh}})$ onto physical units using the scaling relations introduced in BCQM III and the accompanying technical note [3, 2]. In practice this means fixing a physical time step Δt_{phys} and a characteristic displacement scale Δx_{phys} for the probe, and identifying the dimensionless acceleration used in the simulation with

$$a_{\mathrm{phys}}(t) = a_0\, a_{\mathrm{dim}}(t/\Delta t_{\mathrm{phys}}), \qquad a_0 \sim \frac{\Delta x_{\mathrm{phys}}}{\Delta t_{\mathrm{phys}}^2}.$$

The corresponding one-sided acceleration-noise spectra then obey a simple scaling relation of the form

$$S_a^{\mathrm{phys}}(\omega) = a_0^2\, \Delta t_{\mathrm{phys}}\, S_a^{\mathrm{dim}}(\omega\, \Delta t_{\mathrm{phys}}),$$

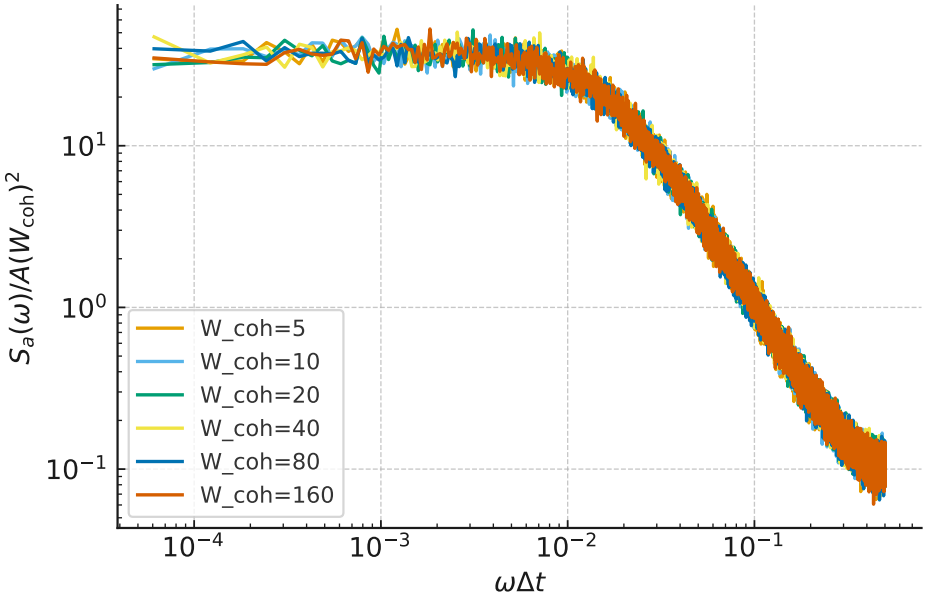

Figure 3: Rescaled dimensionless spectra $S_a(\omega; W_{\rm coh})/A(W_{\rm coh})^2$ for the canonical $W_{\rm coh}$-blind control kernel, plotted against the dimensionless frequency $\omega\Delta t$. Over the band $0.01 \le \omega\Delta t \le 0.3$ the root-mean-square fractional deviation from the band mean is $\simeq 0.11$ and the maximum deviation is $\lesssim 0.26$, while larger departures are confined to the high-frequency region near the lattice cutoff $\omega \sim 1/\Delta t$, indicating an approximate universality of spectral shape for the control model in the low-to-mid-frequency regime.

where $S_a^{\rm dim}$ is the dimensionless spectrum returned by the simulation. This allows us to express the low-frequency noise level as $S_a^{1/2}(\omega_{\rm ref})$ in $\mathrm{m\,s^{-2}/\sqrt{Hz}}$ at reference frequencies $\omega_{\rm ref}$ of interest.

We then compare these BCQM noise levels with typical reported noise floors for the chosen platforms, indicating whether the predicted BCQM floor lies well below, comparable to, or above current sensitivities. In the present control study, where the kernel is deliberately $W_{\rm coh}$-blind, this comparison should be regarded as a baseline exercise: it shows how any future BCQM-induced scaling of $A_a(W_{\rm coh})$ would map into the usual experimental figures of merit.

On this basis we estimate a thermal crossover temperature $T_{\rm crit}$ for each benchmark: the temperature below which further cooling would no longer reduce the observed noise because the BCQM contribution would dominate over thermal fluctuation forces. Operationally, we obtain $T_{\rm crit}$ by equating the BCQM contribution $S_a^{\rm BCQM}(\omega_{\rm ref})$ with a standard thermal acceleration-noise model $S_a^{\rm thermal}(\omega_{\rm ref}, T)$ appropriate to the platform (for example a Brownian-motion model for a mechanical resonator with an effective damping or integration time τ). Since $S_a^{\rm thermal}$ typically scales linearly with T in the low-temperature regime of interest, this equality defines $T_{\rm crit}$ up to an order-unity factor determined by the benchmark parameters and τ (for concreteness we take $\tau \simeq 1\,\mathrm{s}$ in the benchmarks below); in particular $T_{\rm crit} \propto \tau$, so readers can rescale our illustrative values to their own devices. Crucially, the BCQM noise floor is independent of temperature for $T \ll T_{\rm crit}$, in contrast to thermal fluctuations. For $T > T_{\rm crit}$ the BCQM contribution remains present but becomes subdominant to the ordinary thermal noise, so in practice the intrinsic floor is then hidden beneath the thermal background. Where space permits we summarise the result in a simple frequency–temperature exclusion-style plot, highlighting the region in which BCQM inertial noise would be the leading contribution.

To anchor these scalings we consider three illustrative benchmarks. The first is a nanomechanical resonator with mass $m = 10^{-14}\,\mathrm{kg}$ (a ten-picogram oscillator). Using a representative coherence

Table 1: Illustrative BCQM inertial-noise benchmarks for the canonical W_{coh}-blind control kernel, using $\Delta t_{\mathrm{phys}} = 10^{-8}\,\mathrm{s}$, a dimensionless low-frequency plateau $S_a^{\mathrm{dim}} \simeq 50$, and $\tau = 1\,\mathrm{s}$ in the definition of T_{crit}. The hop scale is taken as $\Delta x_{\mathrm{phys}} \sim \sqrt{\hbar \Delta t_{\mathrm{phys}}/m}$ for all three benchmarks.

Benchmark	m [kg]	Δt_{phys} [s]	Δx_{phys} [m]	a_0 [$\mathrm{m\,s^{-2}}$]	$S_a^{1/2}$ [$\mathrm{m\,s^{-2}/\sqrt{Hz}}$]	T_{crit} [K]
Cold atom (Rb-87)	1.4×10^{-25}	1.0×10^{-8}	2.7×10^{-9}	2.7×10^{7}	1.9×10^{4}	9.5×10^{5}
Nanomechanical resonator	1.0×10^{-14}	1.0×10^{-8}	1.0×10^{-14}	1.0×10^{2}	7.3×10^{-2}	9.5×10^{5}
Macroscopic test mass	4.0×10^{1}	1.0×10^{-8}	1.6×10^{-22}	1.6×10^{-6}	1.1×10^{-9}	9.5×10^{5}

time $W_{\mathrm{phys}} \approx 1\,\mu\mathrm{s}$ and a simulation horizon $W_{\mathrm{sim}} \approx 100$ steps fixes a physical time step $\Delta t_{\mathrm{phys}} \approx 10\,\mathrm{ns}$. Identifying the hop scale with a naive quantum-spread estimate, $\Delta x_{\mathrm{phys}} \sim \sqrt{\hbar \Delta t_{\mathrm{phys}}/m}$, and taking a typical dimensionless low-frequency plateau $S_a^{\mathrm{dim}} \sim 50$ from the control spectra, we obtain an acceleration scale $a_0 \sim 10^2\,\mathrm{m\,s^{-2}}$ and a BCQM acceleration-noise plateau $S_a^{\mathrm{phys}} \sim 5 \times 10^{-3}\,\mathrm{m^2\,s^{-3}}$, corresponding to $S_a^{1/2} \sim 7 \times 10^{-2}\,\mathrm{m\,s^{-2}/\sqrt{Hz}}$ or a few $10^{-3}\,g/\sqrt{\mathrm{Hz}}$.

As a contrasting macroscopic benchmark we take a 40 kg test mass with the same Δt_{phys} and dimensionless plateau. The same construction then yields an acceleration-noise floor $S_a^{1/2} \sim 1 \times 10^{-9}\,\mathrm{m\,s^{-2}/\sqrt{Hz}}$, i.e. of order $10^{-10}\,g/\sqrt{\mathrm{Hz}}$. For comparison we also include in our summary table a single cold atom (Rb-87) treated with the same naive hop-scale prescription; this yields a much larger acceleration-noise level and serves mainly as a sanity check on the underlying assumptions rather than as a serious phenomenological prediction.

These illustrative values are summarised in Table 1. In all three cases the corresponding thermal crossover temperature $T_{\mathrm{crit}} \simeq S_a^{\mathrm{phys}} m\tau/(4k_{\mathrm{B}})$ (with $\tau \sim 1\,\mathrm{s}$ in our examples) lies near $10^6\,\mathrm{K}$. This near mass-independence of T_{crit} is a direct consequence of our deliberately naive hop-scale prescription, in which the WKB-like estimate $\Delta x_{\mathrm{phys}} \sim \sqrt{\hbar \Delta t_{\mathrm{phys}}/m}$ cancels the explicit factor of m in the Brownian expression for T_{crit}; the resulting T_{crit} values should therefore be read as a consistency check on the scaling rather than as sharp phenomenological predictions. So the BCQM contribution behaves as an effectively temperature-independent floor under any realistic laboratory conditions. For the nanomechanical benchmark this floor sits at a few $10^{-3}\,g/\sqrt{\mathrm{Hz}}$, while for the macroscopic test mass it falls in the nano-$g/\sqrt{\mathrm{Hz}}$ regime. A naive application to a single cold atom would, however, clearly overpredict existing interferometer sensitivities and confirms that the microscopic BCQM hop scale must be chosen more carefully for light probes than this simple estimate suggests.

These benchmarks should therefore be read as baseline BCQM floors for the W_{coh}-blind control kernel; any genuine W_{coh}-dependence in future kernels would shift these values, potentially in a platform-dependent way.

6 Results: simple cluster models and centre-of-mass noise

To probe how BCQM inertial noise behaves for small bound systems we extend the control kernel to a minimal cluster toy built from a finite number of probe threads. In this first implementation we deliberately take the probes to be independent and identically distributed: each thread follows the same W_{coh}-blind OU-like kernel used in the single-probe study, and a "cluster of size N" is simply a set of N such threads evolved in parallel. The only collective dynamical quantity we construct is the centre-of-mass (COM) acceleration,

$$a_{\mathrm{COM},n} = \frac{1}{N} \sum_{i=1}^{N} a_{i,n}, \tag{1}$$

so this toy provides a baseline against which more realistic, correlated cluster models can be compared in future work.

For each cluster size $N \in \{2, 4, 8, 16, 32, 64, 128\}$ we generate ensembles of COM trajectories with the same numerical parameters as in the single-probe scan and compute their acceleration-noise spectra in the same way. From the ensemble-averaged COM spectra we extract an overall amplitude $A_{\mathrm{COM}}(N)$ and spectral centroid $\omega_{c,\mathrm{COM}}$ using the same conventions as in section 4. The resulting amplitudes are shown in Fig. 4 on log–log axes, together with a reference $N^{-1/2}$ scaling. A linear fit of $\log_{10} A_{\mathrm{COM}}$ against $\log_{10} N$ yields a slope

$$A_{\mathrm{COM}}(N) \propto N^{\alpha}, \qquad \alpha = -0.495 \pm 0.001, \tag{2}$$

with $R^2 \simeq 0.99997$, and the product $A_{\mathrm{COM}}(N)\sqrt{N}$ is constant to within a few per cent across the entire range $N = 2$–128. The COM spectral centroid $\omega_{c,\mathrm{COM}}$ remains essentially independent of N, indicating that the shape of the inertial-noise spectrum is the same for all cluster sizes in this toy model and only the overall amplitude changes.

These findings are fully consistent with the macroscopic expectation for N independent probes: because the COM acceleration is an average over N identical and uncorrelated contributions, its variance (and hence its noise amplitude) should fall as $1/\sqrt{N}$. In the present BCQM IV_b context the main role of this cluster toy is therefore to calibrate the numerical machinery and our definitions of COM inertial noise. It establishes a simple, quantitative baseline — an essentially perfect $N^{-1/2}$ suppression of the COM amplitude with N and an N-independent spectral shape — against which more structured, W_{coh}-dependent cluster kernels can be tested in future work. A more realistic treatment of entangled clusters in the configuration-space sense developed in BCQM IV is left to subsequent papers.

At the opposite extreme, a fully correlated ("rigid") cluster in which all probes share the same acceleration history would have a COM spectrum whose W_{coh}–dependence mirrors that of a single effective probe, with the overall acceleration amplitude suppressed by the total mass of the cluster rather than by independent averaging. In that sense the independent-probe baseline reported here and the rigid limit bracket the range between uncorrelated and fully correlated few-body behaviour that will be explored in more realistic, W_{coh}–sensitive cluster kernels in the gravitational BCQM V setting.

7 Discussion and outlook

7.1 Summary of numerical findings

In this companion paper BCQM IV_b we have deliberately restricted attention to a minimal, W_{coh}-blind control kernel on a single thread, implemented in the code package `bcqm_toy_3`. The primary aim has been to validate the simulation–and–analysis pipeline illustrated in sections 3 and 4, rather than to extract a final physical prediction for the inertial-noise spectrum.

Within this restricted setting the numerical findings can be summarised succinctly. First, for all coherence horizons in the scan $W_{\mathrm{coh}} \in [5, 160]$ (in units of hops) the dimensionless acceleration spectra $S_a(\omega; W_{\mathrm{coh}})$ produced by `bcqm_toy_3` are smooth, free of obvious numerical artefacts in the frequency band of interest, and stable under reasonable variations of the numerical parameters (trajectory length, ensemble size, and windowing choices). Second, the inertial-noise amplitude $A_a(W_{\mathrm{coh}})$ extracted from these spectra shows no statistically significant dependence on W_{coh} over the scanned range: log–log fits of $A_a(W_{\mathrm{coh}}) \propto W_{\mathrm{coh}}^{-\beta}$ yield values of β consistent with zero within the quoted uncertainties. Third, when these control results are viewed alongside the archived toy models described in Appendix A, they confirm that the pipeline behaves as intended. When a non-trivial W_{coh}–dependence is built explicitly into the microscopic update rule, the

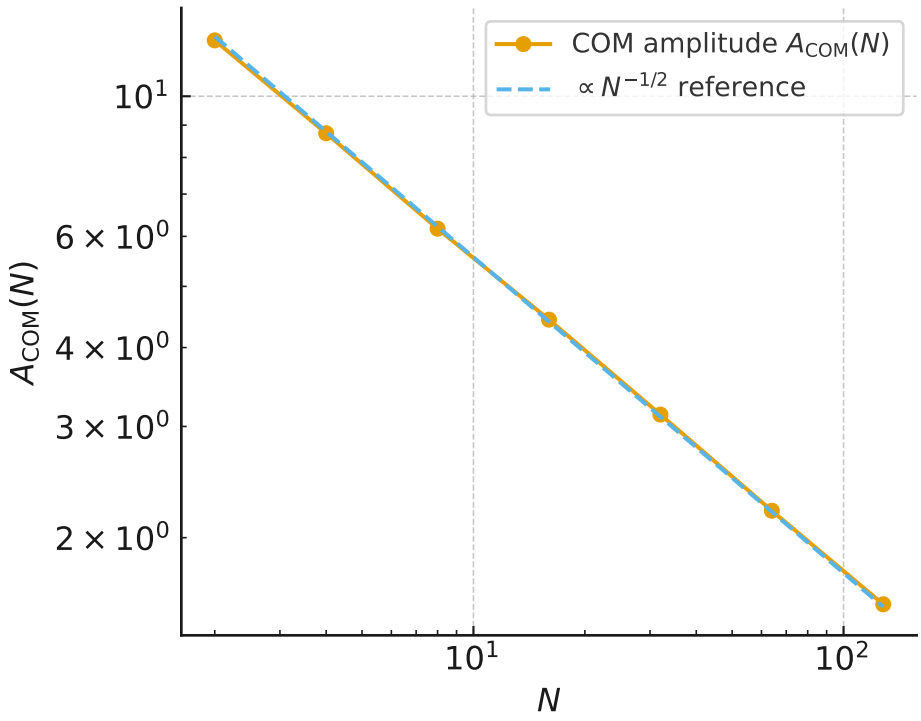

Figure 4: Centre-of-mass acceleration amplitude $A_{\mathrm{COM}}(N)$ for the cluster toy as a function of the number of probes N, on log–log axes. Points show the measured amplitudes from the N-scan and the dashed line is a reference $N^{-1/2}$ scaling with normalisation fixed by $\langle A_{\mathrm{COM}}(N)\sqrt{N}\rangle$. The best-fit slope is -0.495 with $R^2 \simeq 0.99997$, confirming the expected $A_{\mathrm{COM}}(N) \propto N^{-1/2}$ behaviour for this independent-probe toy model.

analysis recovers a corresponding non-zero β; conversely, for the stationary W_{coh}-blind kernel of `bcqm_toy_3` it reports $\beta \simeq 0$ and a nearly constant $A_a(W_{\mathrm{coh}})$. The numerical infrastructure developed here can therefore be taken as a reliable baseline for more elaborate, BCQM-motivated kernels in which W_{coh} enters dynamically.

7.2 Comparison with BCQM IV expectations

BCQM IV argues, at a heuristic level, that the coherence horizon W_{coh} should enter the effective inertial response of bounded systems, and that suitably chosen microscopic kernels ought to generate a characteristic W_{coh}–dependence in the centre-of-mass noise spectrum. The present paper does not yet attempt to identify that physical kernel. Instead, it isolates the logically prior question: does the numerical machinery itself introduce any spurious W_{coh}-scaling, or can we cleanly separate genuine BCQM effects from analysis artefacts?

The control results obtained with the stationary, W_{coh}-blind kernel of `bcqm_toy_3` are entirely consistent with the latter, more optimistic, outcome. Since W_{coh} does not appear in the local update rule, BCQM does not require any particular scaling of $A_a(W_{\mathrm{coh}})$ in this case, and a null result $\beta \simeq 0$ is the expected behaviour. Precisely this pattern is observed: within uncertainties the amplitudes are flat across the scanned range, and the inferred exponent is statistically compatible with zero. At the same time, the archived toy dynamics in Appendix A demonstrate that, when a W_{coh}-dependence is engineered into the microscopic dynamics, the same pipeline correctly recovers a non-trivial β.

Taken together, these observations support the working assumption of BCQM IV that W_{coh}-

dependent inertial noise, if present in more realistic kernels, will originate in the underlying hop statistics rather than in the analysis procedure. The role of BCQM IV_b is therefore to provide a controlled numerical baseline: it establishes the behaviour of the simplest W_{coh}-blind kernel, quantifies the null result for β, and prepares the ground for subsequent studies in which the BCQM heuristics are encoded explicitly into W_{coh}-sensitive kernels and into small bound clusters.

7.3 Implications for BCQM V

Finally, we outline how the inertial-noise spectra obtained here feed into the planned BCQM V analysis of stochastic gravitational lensing and emergent curvature. The emphasis will be on how a well-characterised inertial noise floor, together with a clear scaling structure, can serve as input to models in which fluctuations of event density and cluster structure manifest as curvature fluctuations at larger scales.

Appendices

Appendix A Numerical checks - code validation

In this appendix we collect the minimal stochastic models used to validate the inertial-noise pipeline (trajectory simulation, spectral estimation, and amplitude fitting). They serve two roles: (i) to demonstrate that the code can recover a non-trivial W_{coh}–scaling when it is deliberately built into the microdynamics, and (ii) to show that the pipeline does not artificially manufacture a power law when none is present. The first two branches are archived "toy" models used as positive and negative controls. The third is the canonical, BCQM-motivated control toy used for the results quoted in the main text.

A.1 Toy dynamics branch (21–11–25)

The first code branch (folder `toy_dynamics_branch_21-11-25`) implements two simple random-walk models on a 1D chain. They are not intended to be BCQM-realistic, but rather to stress-test the analysis pipeline.

- *Explicitly W_{coh}–scaled step model.* Here the effective step statistics are chosen such that the coarse-grained inertial-noise amplitude $A(W_{\mathrm{coh}})$ necessarily carries a power-law dependence. Concretely, the position x_n on a 1D chain is updated as

$$x_{n+1} = x_n + \sigma(W_{\mathrm{coh}})\,\xi_n, \qquad \sigma(W_{\mathrm{coh}}) = \sigma_0 W_{\mathrm{coh}}^{-1/2},$$

  with $\xi_n \sim \mathcal{N}(0,1)$ independent and identically distributed and fixed σ_0. This enforces a step-size scaling $dx \propto W_{\mathrm{coh}}^{-1/2}$ and hence a coarse-grained amplitude $A(W_{\mathrm{coh}}) \propto W_{\mathrm{coh}}^{-1/2}$. Running the full pipeline (ensemble generation, spectra, and log–log regression) yields a fitted exponent

$$A(W_{\mathrm{coh}}) \propto W_{\mathrm{coh}}^{-\beta}, \qquad \beta \simeq 0.7,$$

  with uncertainties consistent with the imposed scaling. This serves as a positive control: the code can detect a genuine W_{coh}–dependence when it is built into the microdynamics.

- *Persistent random walk model.* The second toy in this branch is a nearest-neighbour random walk with a simple persistence parameter $\rho = \exp(-\Delta t/W_{\mathrm{coh}})$, so that the probability of repeating the previous step is $\frac{1}{2}(1+\rho)$. In this case W_{coh} controls only the short-range

correlations between successive steps, but does not significantly alter the overall roughness of the trajectory. The extracted amplitude $A(W_{\mathrm{coh}})$ is essentially flat across the scan, and the fitted exponent is

$$\beta \simeq 0 \quad \text{(consistent with no } W_{\mathrm{coh}} \text{ scaling)}.$$

This provides a negative control: the pipeline does not spuriously create a power law when only weak local correlations are present.

A.2 BCQM rudder toy v1

The second branch (folder `bcqm_rudder_toy_v1`) implements a BCQM-motivated "rudder + interruption" kernel on a 1D chain:

- Each trajectory records a single probe on a discrete chain with positions x_n.
- The internal state includes the last realised displacement $\Delta x_n = x_n - x_{n-1}$, whose sign defines a local *rudder* $s_n \in \{-1, 0, +1\}$: "I was there, now I am here".
- At each step, in the absence of interruptions, the hop probabilities to the right and left neighbours are tilted by the rudder,

  $$p_{n\to n\pm 1} = \frac{1}{2}(1 \pm \varepsilon s_n),$$

  with a small bias $\varepsilon \ll 1$.
- Interruptions, controlled on average by a coherence-horizon parameter W_{coh}, sporadically reset the rudder to $s_n = 0$, after which the local motion resumes its biased form.

This toy is more faithful to the BCQM picture in that it encodes a minimal "memory" of the last realised hop, periodically erased on a timescale set by W_{coh}. However, the numerical results show that, over the ranges scanned, the inferred amplitudes $A(W_{\mathrm{coh}})$ do not exhibit a clean power law. This is an important structural observation: a very conservative, local BCQM-style kernel in which W_{coh} enters only as a reset timescale for a simple rudder rule does not automatically generate a strong $A(W_{\mathrm{coh}})$ power law. In random-walk terms the horizon controls the correlation length of the motion—by erasing the rudder it randomises the heading—but leaves the single-step variance and long-time diffusion constant essentially independent of W_{coh}. The integrated acceleration variance, and hence the extracted amplitude $A(W_{\mathrm{coh}})$, therefore remain approximately flat across the scan. Finite coherence horizons are necessary in the BCQM picture, but a non-trivial inertial-noise scaling depends sensitively on *how* W_{coh} is realised in the microscopic hop statistics; horizons that only modulate short-range correlations do not by themselves enforce a scale-dependent inertial amplitude.

A.3 Canonical control toy `bcqm_toy_3`

The third and current branch (folder `bcqm_toy_3`) is the canonical control model used for the quantitative tests in the main text. It implements a simple, stationary acceleration kernel on a single thread, deliberately *blind* to W_{coh}:

- Time is discretised with a fixed step Δt, and each trajectory consists of N steps.
- The dynamical variable is the acceleration a_n along the thread, updated by an Ornstein–Uhlenbeck–type rule

  $$a_{n+1} = (1 - \gamma)\, a_n + \sigma\, s\, \xi_n,$$

  where $0 < \gamma \ll 1$ is a fixed relaxation parameter, σ is a fixed noise scale, $s \in \{+1, -1\}$ is a "sign mode" choice, and $\xi_n \sim \mathcal{N}(0, 1)$ are independent Gaussian kicks.

- Crucially, the kernel parameters (γ, σ, s) are *independent* of W_{coh}. The coherence horizon enters only through the label of the scan: we generate ensembles of trajectories for a list of values $W_{\mathrm{coh}} \in \{5, 10, 20, 40, 80, 160\}$ and process each ensemble in the same way.
- For each W_{coh} the code computes the one-sided power spectral density $S_a(\omega)$ of the acceleration, extracts a total amplitude

$$A(W_{\mathrm{coh}}) = \left(\int_0^\infty S_a(\omega)\, \mathrm{d}\omega \right)^{1/2},$$

  and a characteristic frequency ω_c from the spectral centroid. The resulting $(W_{\mathrm{coh}}, A, \omega_c)$ triples are stored to disk and used for the log–log fit.

With a representative configuration ($\Delta t = 1$, $N = 16384$, 64 trajectories per W_{coh}, fixed random seed, and either sign mode $s = \pm 1$) the measured amplitudes cluster tightly around $A \approx 2.3$ across the full scan. A log–log fit of the form

$$A(W_{\mathrm{coh}}) \propto W_{\mathrm{coh}}^{-\beta}$$

then yields

$$\beta \simeq 4 \times 10^{-4} \quad \text{with uncertainty of order } 7 \times 10^{-4},$$

that is, statistically consistent with $\beta = 0$. Flipping the sign mode s reverses the sign of a_n but leaves the power spectra unchanged, and hence gives identical (A, ω_c) pairs and fitted β.

This branch is therefore a clean, BCQM-motivated control: a stationary kernel with no explicit W_{coh} dependence produces $A(W_{\mathrm{coh}})$ consistent with a constant, and the pipeline correctly reports $\beta \approx 0$ within errors. Subsequent W_{coh}-sensitive kernels can be compared directly against this baseline.

A.4 Cluster toy for centre-of-mass noise

For the simple cluster results reported in section 6 we implemented a separate code branch (folder `bcqm_cluster_toy`) that extends the canonical single-thread control kernel to a finite number of probes. In this branch each probe follows the same W_{coh}-blind OU-like acceleration kernel as in `bcqm_toy_3`, and a cluster of size N is modelled as N such threads evolved in parallel with independent Gaussian kicks. The only collective observable we construct is the centre-of-mass (COM) acceleration,

$$a_{\mathrm{COM},n} = \frac{1}{N} \sum_{i=1}^{N} a_{i,n}, \tag{3}$$

so that the COM inherits any correlations induced by the microscopic kernel without introducing an explicit binding interaction at this stage.

The driver script for this branch (`cluster_simulate.py`) takes a list of cluster sizes $N \in \{2, 4, 8, 16, 32, 64, 128\}$ and, for each value, generates ensembles of COM trajectories with the same numerical parameters $(\Delta t, N_{\mathrm{steps}}, n_{\mathrm{ensembles}})$ as in the single-probe scan. For each N it computes an ensemble-averaged one-sided COM spectrum $S_{a,\mathrm{COM}}(\omega; N)$ and extracts a COM amplitude $A_{\mathrm{COM}}(N)$ and spectral centroid $\omega_{c,\mathrm{COM}}$ using the same conventions as in the main text. The outputs are stored as a set of `cluster_N{N}.npz` files (frequencies, spectra, and metadata) plus a summary CSV (`amplitude_scaling_COM.csv`) containing the pairs $(N, A_{\mathrm{COM}}, \omega_{c,\mathrm{COM}})$ plotted in figure 4.

A log–log regression of $A_{\mathrm{COM}}(N)$ against N yields

$$A_{\mathrm{COM}}(N) \propto N^{\alpha}, \qquad \alpha = -0.495 \pm 0.001, \tag{4}$$

with $R^2 \simeq 0.99997$, and the product $A_{\mathrm{COM}}(N)\sqrt{N}$ is constant at the level of $\simeq 17.6$ with a scatter below 1 % across the entire range $N = 2$–128. The COM spectral centroid $\omega_{c,\mathrm{COM}}$ is essentially independent of N at the few-per-mille level. These results confirm that, for this independent cluster toy, the COM inertial-noise spectrum retains the same shape as the single-probe spectrum while its amplitude is suppressed almost exactly as $N^{-1/2}$. As in the W_{coh}-blind single-probe case, the main role of this branch is to provide a quantitative baseline: it demonstrates that the analysis pipeline recovers the expected $N^{-1/2}$ suppression when averaging over independent probes, so that any departures from this behaviour in future correlated or W_{coh}-sensitive cluster kernels can be unambiguously attributed to the modified microdynamics rather than to analysis artefacts. All toy models and analysis scripts described in this appendix are implemented in the BCQM_IV_b companion code package [12].

References

[1] Peter M. Ferguson. *Boundary-Condition Quantum Mechanics IV: Inertial Noise and the Emergent Action*. BCQM IV working draft. 2025. DOI: 10.5281/zenodo.17650149. URL: https://doi.org/10.5281/zenodo.17650149.

[2] Peter M. Ferguson. *BCQM Technical Note: Emergent Inertia and Invariant Action from Graph-Phase Dynamics*. BCQM technical note, working draft. 2025. DOI: 10.5281/zenodo.17650235. URL: https://doi.org/10.5281/zenodo.17650235.

[3] Peter M. Ferguson. *Boundary-Condition Quantum Mechanics III: A Stochastic Growth Model for Causal Event Chains and the Emergence of Inertia*. 2025. DOI: 10.5281/zenodo.17632453. URL: https://doi.org/10.5281/zenodo.17632453.

[4] Peter M. Ferguson. *Boundary-Condition Quantum Mechanics (BCQM)*. 2025. DOI: 10.5281/zenodo.17191306. URL: https://doi.org/10.5281/zenodo.17191306.

[5] Peter M. Ferguson. *Boundary-Condition Quantum Mechanics II: From Quantum Events to Spacetime*. 2025. DOI: 10.5281/zenodo.17398294. URL: https://doi.org/10.5281/zenodo.17398294.

[6] Peter M. Ferguson. *Minimal amplitude-first primitives for BCQM: events, directed edges, and complex amplitudes with a single hop-bounded selection rule*. 2025. DOI: 10.5281/zenodo.17495038. URL: https://doi.org/10.5281/zenodo.17495038.

[7] G.C. Ghirardi, A. Rimini and T. Weber. 'Unified dynamics for microscopic and macroscopic systems'. In: *Physical Review D* 34.2 (1986), pp. 470–491. DOI: 10.1103/PhysRevD.34.470.

[8] A. Bassi and G. C. Ghirardi. 'Dynamical reduction models'. In: *Physics Reports* 379.5-6 (2003), pp. 257–426. DOI: 10.1016/S0370-1573(03)00103-0.

[9] Peter M. Ferguson. *Boundary-Condition Quantum Mechanics (BCQM)*. Preprint : https://doi.org/10.5281/zenodo.17191306. 2025. DOI: 10.5281/zenodo.17191307. URL: https://doi.org/10.5281/zenodo.17191306.

[10] V. Gorini, A. Kossakowski and E. C. G. Sudarshan. 'Completely positive dynamical semigroups of N-level systems'. In: *Journal of Mathematical Physics* 17.5 (1976), pp. 821–825. DOI: 10.1063/1.522979.

[11] Göran Lindblad. 'On the Generators of Quantum Dynamical Semigroups'. In: *Communications in Mathematical Physics* 48.2 (1976), pp. 119–130. DOI: 10.1007/BF01608499. URL: https://doi.org/10.1007/BF01608499.

[12] Peter M. Ferguson. *BCQM IV_b companion code v1.0.0*. GitHub+Zenodo snapshot of the BCQM_IV_B simulation and analysis code. 2025. DOI: 10.5281/zenodo.17815304. URL: https://doi.org/10.5281/zenodo.17815304.